International Journal of Applied Earth Observation and Geoinformation 8 (2006) 173–187

INTERNATIONAL JOURNAL OF APPLIED EARTH OBSERVATION AND GEOINFORMATION

www.elsevier.com/locate/jag

Biomass mapping using forest type and structure derived from Landsat TM imagery

J.E. Luther [a,*], R.A. Fournier [b], D.E. Piercey [a], L. Guindon [c], R.J. Hall [d]

[a] *Natural Resources Canada, Canadian Forest Service-Atlantic Forestry Centre, University Drive, P.O. Box 960, Corner Brook, NL, Canada A2H 6J3*

[b] *Centre de Recherches et applications en télédétection (CARTEL), Université de Sherbrooke, Sherbrooke, QC, Canada J1K 2R1*

[c] *Natural Resources Canada, Canadian Forest Service-Laurentian Forestry Centre, 1055 du P.E.P.S., P.O. Box 3800, Sainte-Foy, QC, Canada G1V 4C7*

[d] *Natural Resources Canada, Canadian Forest Service-Northern Forestry Centre, 5320-122nd Street, Edmonton, AB, Canada T6H 3S5*

Received 18 February 2005; accepted 19 September 2005

Abstract

A method for mapping forest biomass was developed and tested on a study area in western Newfoundland, Canada. The method, BIOmass from Cluster Labeling Using Structure and Type (BioCLUST), involves: (i) hyperclustering a Landsat TM image, (ii) automatically labeling the clusters with information about forest type and structure, and (iii) applying stand-level equations that estimate biomass as a function of height and crown closure within forest species-type classes. BioCLUST was validated with biomass values measured at geo-referenced field plots and mapped across the study area using an existing forest management photo-inventory. Root mean square error (RMSE) values ranged from 43 to 79 tonnes/ha, and were lowest for intermediate height classes when validated with field plots. Overall bias was negative at 10 tonnes/ha compared with a negative bias of 3 tonnes/ha estimated for the photo-inventory. Validation of the biomass map gave RMSE values of 37–47 tonnes/ha and overall landscape biomass estimates within 0.4% of biomass mapped by the photo-inventory. BioCLUST offers an alternative to other biomass mapping methods when scene-specific plot data are limited and a photo-inventory is available for a representative portion of a Landsat scene.

Keywords: Boreal environment; Classification; Forest biomass; Forest inventory; Geographical information systems; Landsat TM

1. Introduction

Forest biomass, the dry mass of the aboveground portion of live trees per unit of area (Bonnor, 1985), is a basic forest attribute that is linked to many forest ecosystem processes. It is an important input to global change and productivity models and is needed to assess carbon stocks and the contribution of forests to the global carbon cycle (Penner et al., 1997). Increasingly, aggregate estimates of biomass and other inventory attributes are required on a national scale (Lowe et al., 1994, 1996a,b; Penner et al., 1997; Fang et al., 1998; Brown et al., 1999) to meet the reporting requirements of national and international initiatives such as criteria and indicators of sustainable forest management (Canadian Council of Forest Ministers, 1997) and in response to the commitments stemming from the Kyoto Protocol (Nabuurs et al., 2000).

* Corresponding author. Tel.: +1 709 637 4917; fax: +1 709 637 4910.
E-mail address: jluther@nrcan.gc.ca (J.E. Luther).

0303-2434/$ – see front matter
doi:10.1016/j.jag.2005.09.002

Presently, spatially explicit estimation of forest biomass in Canada relies heavily on well-established forest inventory programs. Stand-level forest inventories provide the state of forests at a scale required for operational planning (e.g., Delaney and Osmond, 1977). Usually, they consist of detailed plot measurements of individual tree attributes, as well as digital maps interpreted from aerial photographs (hereafter referred to as photo-inventory maps) that provide a stratification of forest types for timber inventory purposes and regional assessment of the forest resource. In addition to serving as a working tool for forest managers, photo-inventories have been used to derive spatially explicit forest biomass by applying biomass look-up tables or regression equations to forest type and structure information contained within the stand-level maps (Fournier et al., 2003).

Approaches for deriving forest inventory information from satellite remote sensing images can be described under three broad categories (reviewed in Hall et al., 1995). They include: (i) classification algorithms that are most commonly applied to discriminate species composition classes, and (ii) empirical (Cohen and Spies, 1992; Cohen et al., 2001), or (iii) physical models (Woodcock et al., 1994; Gemmell and Varjo, 1999) used to estimate forest structural or biophysical properties. More specifically, satellite-based methods for biomass estimation have included the development of empirical relationships with spectral reflectance or derived indices, such as the normalized difference vegetation index (Dong et al., 2003). In more integrated approaches for classification and modeling (Hall et al., 1997), ancillary data sets (e.g., elevation models, ecosystem classifications, forest inventories) have been used to filter analyses (Kilpelainen and Tokola, 1999), stratify remote sensing analyses by region (Bauer et al., 1994), or be incorporated directly into models or classifications to improve parameter estimation or discrimination (Carpenter et al., 1997). Photo-inventory data sets, in particular, have been integrated with satellite imagery to optimize analysis and generate landscape-level forest inventory attributes (He et al., 1998; Franco-Lopez et al., 2001; Mäkelä and Pekkarinen, 2004). For example, the ''*k*-nearest neighbor'' (*k*-NN) (Fazakas et al., 1999; Reese et al., 2002) has been used to map regional-scale forest inventory information in Finland and Sweden (Franco-Lopez et al., 2001; Tomppo and Halme, 2004) and more recently, to map biomass in a northern boreal forest area in Canada (Beaudoin et al., 2005).

This paper presents a new method, BIOmass from Cluster Labeling Using Structure and Type (BioCLUST), for scaling estimates of biomass from forest inventory plots to the landscape using attributes that can be mapped spatially from Landsat TM imagery. The method involves (i) hyperclustering a Landsat TM image, (ii) automatically labeling the clusters with information about forest type and structure, and (iii) applying stand-level equations that estimate biomass as a function of height and crown closure within forest species-type classes. BioCLUST uses available inventory information on forest type and structure (interpreted from aerial photographs) to optimize the labeling of spectral clusters with forest species type and structure information needed for subsequent biomass estimation. Biomass is assigned to clusters using regression equations derived from forest inventory field plots representative of the particular region.

BioCLUST was developed in the context of the Earth Observation for Sustainable Development of Forests (EOSD) project as an alternative to other biomass mapping methods when scene-specific data are limited, yet inventory over large areas is required (Luther et al., 2002). BioCLUST is compatible with forest management inventories in Canada as it involves extracting those attributes from satellite images (i.e., forest type and structure) that are typically contained in photo-inventory systems. The purpose of this paper is to present details of the method and validation results for a study area in western Newfoundland, Canada.

2. Methods

2.1. Study area description

The study area is delimited by a Landsat scene located on the west coast of the island portion of Newfoundland and Labrador, bounded by the geographic extents 49.78°N, 58.9°W and 47.94°N, 57.05°W (Fig. 1). The total area of the study area is approximately 33,000 km^2, of which one-third is forested. The region contains considerable variation in site conditions due to altitude and proximity to the coast (Meades and Moores, 1994). Most of the study area is in the Corner Brook Subregion of the western Newfoundland Ecoregion (Damman, 1983). This subregion is characterized by hilly to undulating terrain with slates and limestone till as the dominant parent materials. Balsam fir is the dominant forest cover. The eastern section of the study area contains an area of the Northcentral Subregion of the Central Newfoundland Ecoregion. This subregion has a rolling topography

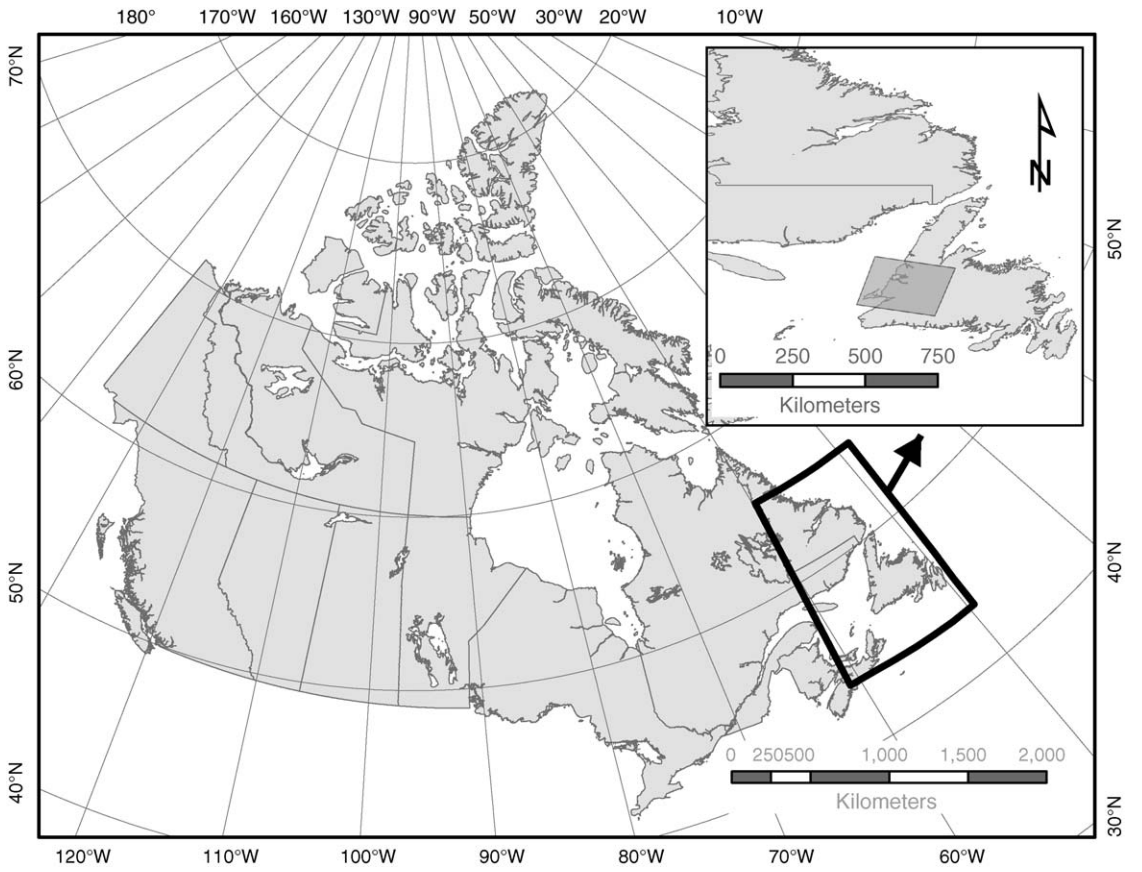

Fig. 1. Geographical location of the Landsat TM image study area in western Newfoundland, Canada.

below 200 m, with nutrient-poor, coarse-textured till prevalent through much of the area. Pure black spruce stands dominate because of the prevalence of fire in the natural history of the subregion.

2.2. Data

2.2.1. Inventory field plot data

The Newfoundland Forest Service provided inventory plot data from their temporary sample plot (TSP) program. Approximately 5000 TSPs were measured by provincial forest inventory crews between 1980 and 1990. Plots were 200 m^2 in size, and were distributed throughout the productive forest areas of Newfoundland and Labrador using a stratified random procedure. Species, height, and DBH were recorded for all the trees with a DBH greater than 9 cm. Species and diameters of trees with DBH between 1 and 9 cm were recorded in subplots that were 40 m^2 in size. Dry weight biomass of all aboveground tree components (hereafter referred as biomass or forest biomass) was estimated for all trees in each plot using allometric tree equations that relate biomass to tree diameter and height (Lavigne, 1982). Species composition, age class, crown closure class, dominant tree height class, and site index were also recorded for each plot.

2.2.2. Photo-inventory maps

Photo-inventory maps (Newfoundland Forest Service, 1991) were interpreted and digitized from 1:12,500 scale aerial photographs acquired between 1986 and 1989. Attributes of forest polygons included species composition, stand height, crown closure, stand age, and site class. Species composition was aggregated into more general forest species types to facilitate forest management applications, including volume estimation and mapping. The provincially defined species types within the region consisted of: black spruce (*Picea mariana* (Mill.) B.S.P.) (bS), balsam fir (*Abies balsamea* (L.) Mill.) (bF), mixed–broadleaf dominant (hS), mixed–coniferous dominant (sH), and white birch (*Betula papyrifera* Marsh.) (wB). At a higher level of aggregation, we combined species-type classes into broader forest cover-type classes: coniferous (C),

broadleaf (D), and mixed forest (M) classes. Stand height was categorized as classes 1 (0–3.5 m), 2 (3.6–6.5 m), 3 (6.6–9.5 m), 4 (9.6–12.5 m), 5 (1.5–15.5 m), 6 (15.6–18.5 m), 7 (18.6–21.5 m), and 8 (>21.6 m). Crown closure was categorized as class 1 or dense (>75%), class 2 or moderate (51–75%), and class 3 or sparse (25–50%).

2.2.3. Stand-level biomass

In previous work (Fournier et al., 2003), the inventory plot data were used to build stand-level biomass equations that estimate biomass for stand attributes that are used in the mapped inventory of Newfoundland and Labrador (i.e., species, projected crown closure, and dominant tree height). First, the biomass of individual trees was summed to calculate biomass at the plot level. Then, plot-level biomass values were extrapolated to total biomass per hectare and related to stand height and crown closure classes for each species type. Error assessment of the regression equations indicated biomass prediction with RMSE values of 38–47 tonnes/ha. These values represented a relative error of 35–43% of the mean biomass of the region.

2.2.4. Satellite image data

Landsat-5 TM data were collected on 4 August 1995 (path/row 005/026). The gray level intensities of the raw TM bands were converted to top-of-atmosphere reflectances using radiometric correction software adopted for the EOSD project (Wulder et al., 2003). The image was orthorectified using a digital elevation model generated from Canadian National Topographic Database (NTDB) elevations. Based on 142 ground control points, average root mean square error was 0.49 pixels with x and y errors of 0.37 and 0.32 pixels, respectively.

2.3. Landsat image classification

2.3.1. Unsupervised clustering

Unsupervised clustering followed methods developed in support of the EOSD land cover implementation program (Wulder et al., 2002, 2003). The detailed procedures began with manual masking of cloud, shadow, and haze and removal of these areas from further processing. Next, the image was stratified into four broad spectral categories of reflectance based on a normalized difference vegetation index (NDVI). The spectral categories included non-vegetated masks for land and no-land, and low reflectance and high reflectance vegetation. The NDVI breakpoints for each mask were determined using a manual approach that involved density slicing to determine ''cut-off'' values. Each NDVI mask was processed using a *K*-means unsupervised clustering algorithm with the following input parameters: number of clusters = 241; movement threshold = 0.1; maximum iterations = 12; number of samples = 50% of pixels under mask. The input channels for the classification included TM bands 1–5 and TM band 7.

2.3.2. Cluster labeling

Forest inventory species and structure were assigned to the spectral clusters according to the distribution of randomly sampled pixels from the photo-inventory overlaid onto the spectral clusters. There were 50 pixels sampled for each forest species and structure class on the landscape. To avoid the problem of mixed pixels affecting the distributions, the boundaries between forest inventory species types were removed prior to selection of the random sample pixels. This was achieved by applying a 3 pixels × 3 pixels buffer between each species-type polygon from the photo-inventory maps. Similarly, in order to account, in part, for the time difference between the photo-inventory (1985–1989) and the image date (1995), all areas that had undergone significant disturbances (insects/fire) and management applications (cutting/precommercial thinning) between the date of the forest inventory and the satellite image (1995) were removed from the potential sample area. More specifically, if the time of disturbance was greater than or equal to the inventory date and less than or equal to the image date, this area was masked. Sampling was based on the original photo-inventory polygons gridded to 30 m × 30 m cells to match the spatial resolution of the Landsat TM image. A restriction was placed on the sampling whereby a given inventory polygon could only be sampled once. The result was a layer of 3770 randomly selected pixels that were considered to be relatively ''pure'' representations of the inventory species type and structure groups. The proportion of random sample points within a cluster characterized the forest species and structure distribution of the cluster. Several cluster labeling approaches were evaluated based on the proportions (e.g., weighted by the class occurrence). We adopted the dominant species type and structure class to label the cluster (Fig. 2) as any other rules tended to average the biomass estimates and degrade the results in the low and high ends of the biomass range.

2.4. Biomass estimation and mapping

Forest biomass was estimated for each pixel by applying look-up tables derived from the regression

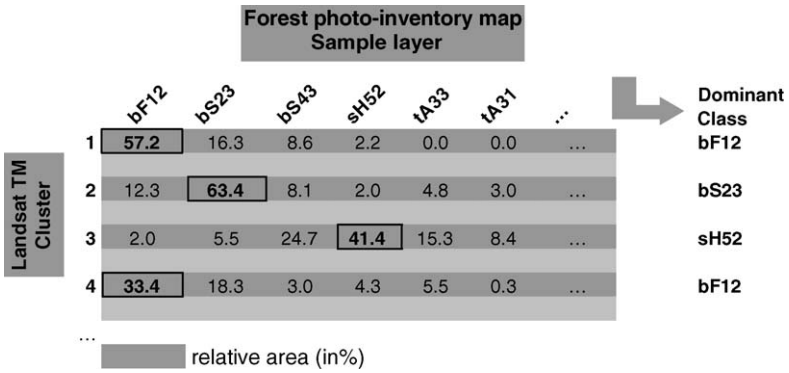

Fig. 2. Graphical representation of the method for labeling clusters with the dominant forest species-type, height, and crown closure classes.

equations of Fournier et al. (2003) to the layer representing the species type and structure class assigned to each cluster. To provide a basis for comparison, the same equations were used to assign biomass values to the species-type, stand height, and crown closure classes contained in the photo-inventory.

2.5. Error estimation

The inventory field plots and photo-inventory maps were used for validation of forest types and biomass estimates generated from the BioCLUST method. Plots or areas of the photo-inventory that experienced disturbances between the period of measurement to the time of the image were not considered in the analysis. This period represented 5–15 years for the plots and 6–9 years for the photo-inventory. The plot attributes and photo-inventory maps were not adjusted according to the expected growth during this timeframe because modeling the growth would have introduced new sources of error and was beyond the scope of this paper.

The categorical and overall accuracy of forest types was computed according to methods outlined by Congalton (1991). Overall species-type accuracy was assessed as a sum of correctly classified field plots divided by the total number of field plots in the error matrix. For comparison purposes, the species classes from the photo-inventory were assessed using the same plots. At the landscape scale, the distribution of forest types and structure classes was assessed relative to the photo-inventory distributions over the entire image area.

The reliability of the biomass estimates was assessed according to the RMSE between the predicted and observed biomass and the associated bias. The RMSE and bias for each species-type, cover-type, height, and crown closure classes were calculated as:

$$\mathrm{RMSE} = \sqrt{\frac{1}{n}\sum_{i=1}^{n}(\hat{e}_i - e_i)^2}$$

where n is the number of plots or pixels, $\hat{e}_i$ the estimated biomass, and e_i is the true value of biomass.

$$\mathrm{Bias} = \bar{e}_1 - \bar{e}_2,$$

where $\bar{e}_1$ is the mean value of the estimated biomass and $\bar{e}_2$ is the mean value of the reference data.

For comparison purposes, the RMSE and bias were also calculated for the photo-inventory map using the geo-referenced field plots. This assessment provided a baseline of biomass prediction capacity using photo-interpreted attributes to which the biomass derived from BioCLUST could be compared in a relative sense.

3. Results

3.1. Accuracy of forest type classes

The overall accuracies for species and cover-type discrimination by the photo-inventory were 86 and 94%, respectively (Table 1). These high accuracies supported the assumption that the photo-inventory provided a reasonable representation of the species-type and cover-type classes over the study area. The overall species-type accuracies of the Landsat classification were much lower at 38%. Given the relatively similar spectral characteristics among species types, the limited ability of the Landsat classification to discriminate among the dominant species (i.e., bF and bS) and mixed forest species types that were predominately broadleaf or coniferous (i.e., hS and sH) was not surprising. Aggregating species to coniferous, broadleaf, and

Table 1
Accuracy of forest type classes from photo-inventory and Landsat TM clusters assessed using inventory field plots[a]

Class	*n*	Photo-inventory (%)		Landsat TM (%)	
		Producer's accuracy[b]	User's accuracy[c]	Producer's accuracy[a]	User's accuracy[b]
By species type[d]					
bF	214	92	91	62	31
bS	93	88	92	32	75
hS	26	64	69	21	27
sH	50	66	62	19	10
wB	22	89	77	26	27
Overall	405	86		38	
By cover type[e]					
C	307	96	97	86	91
D	22	89	77	26	27
M	76	85	84	46	36
Overall	405	94		77	

[a] Forest inventory plot measurement years were between 1980 and 1990 ($n = 405$); photo-inventory based on 1986–1989 aerial photos; Landsat TM image acquired in 1995.
[b] Producer's accuracy is the probability of a reference pixel being correctly classified.
[c] User's accuracy is the probability that a pixel classified on the image represents that category on the ground.
[d] Species-type classes are taken from the provincial forest management inventory; they are defined by the dominant species but may contain components of other species: bF, balsam fir; bS, black spruce; hS, mixed with hardwood dominant; sH, mixed with softwood dominant; wB, white birch.
[e] Cover-type classes are species-type aggregations: C, conifer; D, deciduous; M, mixed.

mixed forest classes improved classification accuracy to 77%. When the photo-inventory was considered to be the source of forest type ''truth'' (Table 2), similar trends in the accuracy of the Landsat image classification results were observed.

Table 2
Accuracy of forest type classes derived from Landsat TM clusters mapped for the study area[a]

	n (pixels)	Producer's accuracy[b]	User's accuracy[b]
Species type[b]			
bF	4095330	66	32
bS	1588459	32	65
hS	258282	12	27
sH	615234	10	9
wB	125107	12	31
Overall	6682412	37	
Cover type[b]			
C	5683789	90	82
D	125107	12	31
M	873516	23	30
Overall	6682412	74	

[a] Photo inventory based on 1986–1989 aerial photos; Landsat TM image acquired in 1995.
[b] See Table 1 for definitions.

3.2. Landscape distribution of forest type and structure

Within the study area, the area covered by the bF species class was underestimated over the landscape by the Landsat classification relative to the photo-inventory and the area covered by bS was overestimated by a comparable amount (Fig. 3a). This was largely due to problems with discrimination between these spectrally similar coniferous species. The relative area distributions of hS, sH, and wB between the photo-inventory and Landsat classification were more similar (Fig. 3a). When the species-type classes were aggregated into forest cover-type classes, the area distributions were within 10% of the total area of the landscape (Fig. 3b).

The photo-inventory and Landsat distributions of height and crown closure classes provided an overall indication of structure across the study area (Fig. 3c and d). Although areas of height classes 4 and 5 were underestimated, the area of class 6 was overestimated by the Landsat classification relative to their respective areas contained in the photo-inventory maps (Fig. 3c). Similarly, crown closure class 1 was overestimated by the Landsat classification, but the adjacent crown closure class 2 was underestimated by approximately the same amount (Fig. 3d).

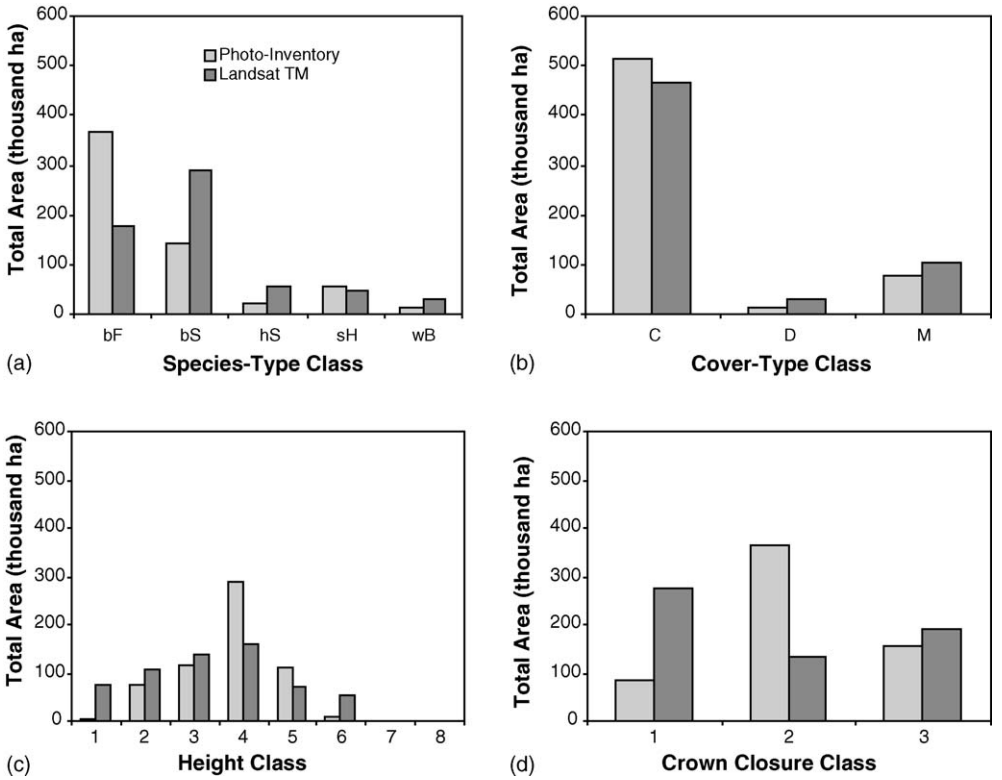

Fig. 3. Area distributions of photo-inventory and Landsat TM maps for forest species-type (a), cover-type (b), height (c), and crown closure (d) classes.

3.3. Validation of biomass estimates

3.3.1. Biomass estimates assessed with inventory field plots

Biomass values of the inventory field plots ranged from 8.3 to 290.4 tonnes/ha (Table 3). Most plots fell within the coniferous cover-type and the bF species-type classes, the dominant forest type in the western Newfoundland landscape. Most plots fell within intermediate height and crown closure classes. There was a wide range of variability in biomass plot estimates within a given species-type, cover-type, height, and crown closure class as indicated by the high standard deviations of the mean biomass estimates for each class.

Not surprisingly, the RMSE values for BioCLUST were higher than those of the photo-inventory when assessed using the field plots (Table 3). The RMSE and bias of the photo-inventory biomass estimates represent the error inherent in applying the biomass look-up tables of Fournier et al. (2003) to the photo-inventory stand maps. Inventory RMSE values ranged from ∼25 to 59 tonnes/ha with the largest errors in the mixed forest cover-type and species-type classes, and the smallest error in the broadleaf classes. Only field plots contained within the study area were assessed here, whereas the tables provided by Fournier et al. (2003) were built and evaluated using plots representative of the entire province of Newfoundland and Labrador.

RMSE values from BioCLUST ranged from approximately 44 to 79 tonnes/ha depending on the species-type, cover-type, height, or crown closure classes assessed. As in the case for the photo-inventory, the highest RMSE values occurred for the mixed forest classes, with the lowest errors for the broadleaf class. Bias was highly negative for the mixed forest classes, indicating that both the photo-inventory and BioCLUST tended to underestimate biomass for these species and cover-type classes. BioCLUST overestimated biomass for the lower height classes (classes 2–3, 3.6–9.5 m) and underestimated biomass for the higher height classes (classes 4–7, 9.6–21.5 m). Moreover, the negative bias increases with the higher height classes and the positive biomass increases with the lower height class. Similarly, the bias for the lowest crown closure class (class 3, 25–50%) was positive at 3.7 tonnes/ha, but the bias for the highest crown closure class (class 1 >75%) was highly negative at ∼39 tonnes/ha. The same general trend was

Table 3
Summary of forest biomass characteristics at field plots and corresponding mean, RMSE, and bias values for photo-inventory and BioCLUST estimates

Class	*n*	Field plots				Photo-inventory			BioCLUST		
		Mean biomass (tonnes/ha)	S.D. (tonnes/ha)	Minimum (tonnes/ha)	Maximum (tonnes/ha)	Mean biomass (tonnes/ha)	RMSE (tonnes/ha)	Bias (tonnes/ha)	Mean biomass (tonnes/ha)	RMSE (tonnes/ha)	Bias (tonnes/ha)
By species type[a]											
bF	214	109.79	45.85	9.6	236.5	111.21	40.02	1.42	98.43	57.62	−11.36
bS	93	101.92	52.65	18.4	233.3	100.19	37.69	−1.74	111.88	69.02	9.95
hS	26	114.53	62.46	22.5	266.2	95.32	58.51	−19.22	85.41	71.26	−29.12
sH	50	119.38	51.18	8.3	290.4	106.34	51.68	−13.04	88.34	79.00	−31.04
wB	22	98.75	39.26	27.3	187.4	95.00	35.39	−3.75	91.78	43.58	−6.98
By cover type[a]											
C	307	107.41	48.06	9.6	236.5	107.87	39.33	0.47	102.51	61.30	−4.90
D	22	98.75	39.26	27.3	187.4	95.00	35.39	−3.75	91.78	43.58	−6.98
M	76	117.72	54.93	8.3	290.4	102.57	54.11	−15.15	87.33	76.44	−30.39
By height[b]											
1											
2	7	49.40	20.30	25.1	80.5	85.51	38.62	36.11	75.22	61.22	25.82
3	104	87.59	40.01	18.4	223.7	94.91	35.49	7.32	92.78	57.01	5.19
4	166	106.34	42.11	22.6	231.3	101.79	39.81	−4.56	98.75	61.08	−7.59
5	103	126.48	54.01	8.3	290.4	119.72	47.89	−6.76	104.97	69.90	−21.50
6	24	158.73	46.94	76.9	266.2	130.48	59.07	−28.25	110.61	78.87	−48.12
7	1	148.90	–	148.9	148.9	173.83	24.93	24.93	91.54	57.36	−57.36
8											
By crown closure[c]											
1	73	126.57	48.79	25.1	233.3	125.60	40.71	−0.97	87.67	61.76	−38.90
2	255	112.40	45.55	18.4	290.4	107.52	40.86	−4.88	106.88	64.14	−5.53
3	77	80.41	49.68	8.3	266.2	83.32	48.12	2.91	84.07	63.66	3.66
All	405	108.87	49.11	8.3	290.4	106.18	42.31	−2.69	99.08	63.63	−9.80

[a] See Table 1 for forest species-type and cover-type definitions.
[b] Stand height is categorized as classes 1 (0–3.5 m), 2 (3.6–6.5 m), 3 (6.6–9.5 m), 4 (9.6–12.5 m), 5 (1.5–15.5 m), 6 (15.6–18.5 m), 7 (18.6–21.5 m), 8 (>21.6 m).
[c] Crown closure is the projected area covered by tree crowns and is categorized as classes 1 (>75%), 2 (51–75%), 3 (25–50%).

observed for the photo-inventory, although the magnitude of the bias was generally lower (2.9 and −1.0 tonnes/ha, respectively). Overall bias for BioCLUST was negative at 10 tonnes/ha compared with a negative bias of 3 tonnes/ha estimated for the photo-inventory.

The average biomass estimated from the photo-inventory and BioCLUST were similar to their field-derived value. The main exceptions appeared in the low and high biomass values. For example, mean biomass values of all data sets for species types of bS, bF, and wB, and cover types of C and D are all within 10%. Meanwhile, species types sH and hS and cover type M diverged more from BioCLUST (reaching an underestimation of about 25%) compared with the photo-inventory baseline (with a difference of 12–21%). This trend was also apparent with mean biomass from structural classes where values for height classes 3–5 are within 20% differences. However, BioCLUST showed significantly more error for low (<3) and high (>5) ends of the height classes compared with the photo-inventory method. On the other hand, mean biomass between the plots and the two methods were similar (approximately 5% difference) for all density classes, with the exception of the dense stands (class 1) for which BioCLUST underestimated values by 31%.

3.3.2. Biomass map assessed with photo-inventory map

When the photo-inventory biomass was used as the ''truth'' source of biomass, thus enabling an assessment of biomass maps at the landscape scale, patterns of RMSE values were similar to those of the field plot assessment. The pattern of negative bias increasing with the higher height class and positive bias increasing with the lower height classes is even more apparent when the

Table 4
Mean, RMSE, and bias values of biomass mapped for the study area and assessed with the photo-inventory map

Class	*n* (pixels)	Mean inventory biomass (tonnes/ha)	Mean BioCLUST biomass (tonnes/ha)	RMSE (tonnes/ha)	Bias (tonnes/ha)
By species type[a]					
bF	4095330	96.52	94.33	44.6	−2.2
bS	1588459	88.64	99.57	47.1	10.9
hS	258282	95.86	91.32	39.5	−4.5
sH	615234	100.27	93.99	43.1	−6.3
wB	125107	94.29	86.28	37.3	−8.0
By cover type[a]					
C	5683789	94.32	95.79	45.3	1.5
D	125107	94.29	86.28	37.3	−8.0
M	873516	98.97	93.20	42.0	−5.8
By height[a]					
1	61794	75.10	81.33	41.5	6.2
2	829524	74.47	85.73	39.4	11.3
3	1276295	82.73	92.20	42.3	9.5
4	3199349	94.91	97.49	45.0	2.6
5	1227341	119.22	99.86	48.7	−19.4
6	86681	139.94	95.41	61.8	−44.5
7	1396	166.92	82.89	93.6	−84.0
8	32	262.73	93.54	173.5	−169.2
By crown closure[a]					
1	933119	115.56	91.42	45.7	−24.1
2	4032590	99.50	97.61	44.0	−1.9
3	1716703	72.96	91.88	46.1	18.9
All	6682412	94.93	95.27	44.8	0.3

[a] See Tables 1 and 3 for forest species-type, cover-type, height, and crown closure class definitions.

full range of height classes were represented on the landscape (Table 4). The overall magnitude of RMSE values was lower because the errors inherent in the photo-inventory estimates of biomass were not incorporated in this assessment. The largest RMSE values occurred for the higher height classes (classes 6–8 with height >15.6 m). Most notable were the very high RMSE (∼170 tonnes/ha) and highly negative bias (−169.2 tonnes/ha) for the highest height class (class 8 with height >21.6 m). This is, in part, because none of the Landsat spectral classes were identified as belonging to height classes 7 or 8; these height classes combined represented less than 0.022% of the forest within the study area.

The BioCLUST map overestimated the area of biomass in the 25–50 and 150–200 tonnes/ha ranges and underestimated the area of the 100–150 tonnes/ha range relative to the inventory map (Fig. 4). This is primarily a result of differences in the areas of forest type and structure classes mapped by the photo-inventory and the Landsat TM image. In particular, the areas of height class 1 and crown closure class 1 were overestimated by BioCLUST relative to the photo-inventory, whereas the areas of intermediate height classes were underestimated (Table 5). Typically, if the area of a particular biomass class range was overestimated, the adjacent range was underestimated, with the exception of the highest class range (150–175 tonnes/ha) which was overestimated. Overall, the area distributions for biomass class ranges of 25 tonnes/ha compared favorably with areas mapped by the photo-inventory. Total forest biomass estimated over the landscape by the photo-inventory was approximately 57.1 million tonnes, and BioCLUST estimated total biomass at approximately 57.3 million tonnes, a biomass difference of approximately 0.4% (Table 5).

Spatially, there was an increased level of variability in the BioCLUST map compared with the map generated by photo-inventory. For the photo-inventory, polygons were spatially generalized through the photo-interpretation process, whereas the BioCLUST map provided estimates for individual pixels (Fig. 5). Therefore, for visual comparison, one must mentally average the pixels values within a polygon to account

Table 5
Area and biomass totals for photo-inventory and BioCLUST maps

Class	Total area (ha)		Total forest biomass (tonnes)		Area difference (%)	Biomass difference (%)
	Photo-inventory map	BioCLUST map	Photo-inventory map	BioCLUST map		
By species type[a]						
bF	368580	177298	35575808	17614680	−51.9	−50.5
bS	142961	290589	12672652	27318662	103.3	115.6
hS	23245	54291	2228240	5230815	133.6	134.8
sH	55371	49541	5552260	4669655	−10.5	−15.9
wB	11260	29698	1061627	2465697	163.8	132.3
By cover type[a]						
C	511541	467887	48248460	44933342	−8.5	−6.9
D	11260	29698	1061627	2465697	163.8	132.3
M	78616	103832	7780499	9900470	32.1	27.2
By height[a]						
1	5561	75506	417679	5791209	1257.7	1286.5
2	74657	105538	5559488	7321208	41.4	31.7
3	114867	135683	9502374	10593872	18.1	11.5
4	287941	160570	27328171	14841590	−44.2	−45.7
5	110461	70610	13169434	10161482	−36.1	−22.8
6	7801	53510	1091711	8590149	585.9	686.9
7	126		20972		−100.0	−100.0
8	3		757		−100.0	−100.0
By crown closure[a]						
1	83981	274116	9704473	28434789	226.4	193.0
2	362933	135527	36113301	16931484	−62.7	−53.1
3	154503	191774	11272812	11933236	24.1	5.9
Total	601417	601417	57090586	57299509	0.0	0.4

[a] See Tables 1 and 3 for forest species-type, cover-type, height, and crown closure class definitions.

for the differences in spatial patterns represented by the two maps (i.e., pixel versus polygon representation of biomass variability). Under those conditions, there was a reasonable correspondence from the high and low biomass regions over the study area.

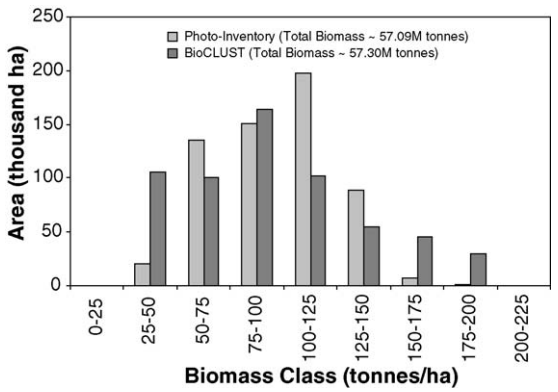

Fig. 4. Area distributions of photo-inventory and BioCLUST maps for biomass class ranges of 25 tonnes/ha.

4. Discussion

4.1. Strengths of the method

A practical method for mapping forest biomass was developed and tested that uses spatial information on forest type and structural attributes of height and crown closure extracted from a satellite image. The correspondence between spectral clusters generated from an unsupervised classification and the dominant class of forest type and structural attributes was established by overlaying representative points selected randomly from a photo-inventory map. Biomass values representative of each forest type and structural class were calculated from regionally distributed field plots and assigned to each cluster, resulting in a forest biomass map of the study area.

The main strengths of the method from a practical perspective are its compatibility with forest inventories in Canada and its limited reliance on scene-specific biomass information (i.e., required for validation

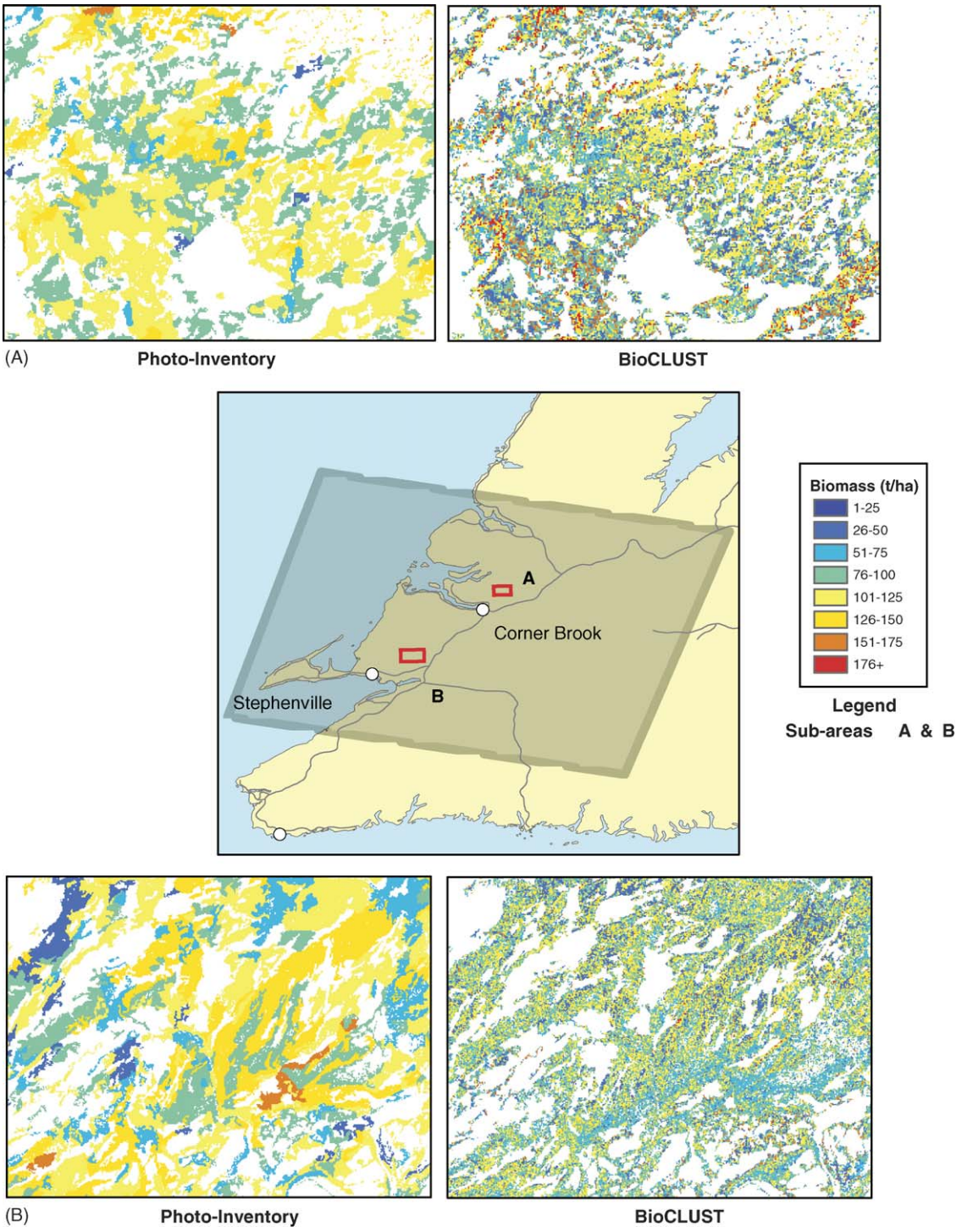

Fig. 5. Comparison of photo-inventory and BioCLUST sub-area maps.

purposes only). The BioCLUST method does not require the use of ground plots within the satellite scene, but it requires photo-inventory coverage within a portion of a satellite image footprint. The method makes use of photo-inventory maps as source data for automatically labeling spectral clusters. BioCLUST complements existing methods (e.g., direct radiometric relationship, *k*-NN, look-up tables, supervised classification) because

it is well adapted to the current constraints prevalent in most Canadian provinces. Such an integrated biomass-mapping approach can improve the utility of traditional photo-inventories by: (i) filling gaps (i.e., areas not mapped for forest management purposes) and (ii) updating biomass in areas that have experienced major disturbances because such areas are represented by the current conditions in the satellite image.

The BioCLUST method was tailored to map biomass and it is, therefore, optimized to provide the best results for that attribute. Aboveground tree biomass, total structural volume and stem volume are very closely related (Penner et al., 1997; Fang et al., 1998), which suggests that BioCLUST could be expanded to stand volume. The applicability for other parameters would need to be explored further as they could require significant changes to the method.

Other strengths of the proposed approach lie in the ability to generate the required attributes from satellite imagery, thus providing increased spatial detail (i.e., on a pixel rather than polygon basis). The approach also provides for a classification based on digital reflectance values with results that may be more comparable across regional jurisdictions. Moreover, biomass estimates derived from satellite images correspond to biomass at the time of image acquisition and have the potential to provide for multi-temporal analyses of biomass, although further development of the methods would be required in this context.

4.2. Sources of error

Several key sources of error may have influenced the results achieved in this study. Generally, these errors are related to: (i) the regression models that relate inventory height and crown closure class to biomass by species, (ii) the photo-inventory maps used for automatic labeling of spectral clusters, and (iii) spatial and temporal discrepancies between the image, field plots, and photo-inventory maps used for validation.

The regression models were used to build biomass look-up tables for height and crown closure class combinations of each species type. These models were influenced by the generalization of three crown closure classes and seven height classes, which resulted in an averaging of predicted biomass values (r^2 = 0.22–0.35; Fournier et al., 2003). This effect meant that variability within a forest species and structure class and extreme biomass values were not captured. Moreover, some species, height, and crown closure class combinations may have contributed to error in the application of the method, this approach is often used for volume estimation in operational forest management.

Sampling the photo-inventory maps for automatic labeling of the spectral clusters provided a good distribution of plots in almost all strata, which is impossible to achieve with existing plot data. However, this approach assumed that the forest inventory maps were ''true'' source data. Although the photo-inventory maps may contain errors, ''expected'' errors were accounted for, in part, by removing buffer zones and disturbed areas between the time of the inventory and the image prior to sampling. Therefore, the BioCLUST method only used what is expected to be the most reliable information contained in the photo-inventory maps. The high classification accuracies of the species types in the photo-inventory supported our assumption that the photo-inventory was reliable for this application.

The validation data likely contained errors that influenced the results achieved. For example, the difference in timing of field plot measurement and image acquisition ranged from 5 to 15 years and may have been a source of error for the plot-level validation. The natural growth of plot attributes was not accounted for within the framework of this study because growth models were not readily available, their development was beyond the scope of this paper, and modeling the growth would have introduced new sources of error in the validation. Similarly, the time discrepancy between the image acquisition and photo-inventory may have contributed to the landscape-level error assessment results. The photo-inventory used in this application represented a typical inventory (6–9 years old). ''Growing'' the inventory stand maps may have made the photo-inventory and the image more correspondent, however, a well-defined method for accomplishing this was not available. Other than accounting for the major forest disturbances by masking, we did not account for other changes (i.e., regular growth of the stands) over the 6–9-year period. Within this region, forest inventories within 10 years are considered ''current'' for planning purposes.[1] Therefore, we did not consider the discrepancy between the photo-inventory and image date to be a highly significant source of error in the application of the method or the validation assessment at the landscape scale.

[1] Harris, D., personal communication, Newfoundland Forest Service, July 2005.

Another limitation of the photo-inventory maps for validation was a result of differences in the mapping process between inventory maps and satellite images. Inventory attributes were determined by stratifying the landscape using an aerial photo-interpretation process. The image analysis was performed on a pixel basis and thus the spatial unit for aggregation was not directly comparable. This spatial discrepancy was clearly evident in the biomass maps generated from the photo-inventory and BioCLUST method (Fig. 5). Although the mapped results may have been non-correspondent at a pixel level, aggregation of values at a common spatial unit may have resulted in a reduction in the overall errors.

The validation results demonstrated that BioCLUST estimates generally had higher RMSE and bias values than the corresponding photo-inventory estimates. BioCLUST estimates for low crown closure stands suffered due to the influence of the understorey on the spectral signal, whereas dense stands were likely affected by the well-known saturation effect. Photo-interpreters use other visual cues such as tone, texture, pattern, and location–association to assess structure, thus understorey and saturation effects were less significant in the photo-inventory estimates.

4.3. Comparison with other approaches

Similar results were achieved using other methods applied on the same study area and using the same data sets.[2] In addition to BioCLUST, the methods compared include: (i) direct radiometric relationships (DRR), (ii) *k*-nearest neighbors (*k*-NN), and (iii) land cover classification (LCC) with the application of biomass look-up tables applied to each cover-type class. Considering the RMSE assessed with field plots, the DRR, *k*-NN, BioCLUST, and LCC methods provided average RMSE values of 59, 59, 58, and 76 tonnes/ha, respectively. Considering the RMSE assessed with an inventory baseline map, the BioCLUST method produced the lowest RMSE (41 tonnes/ha) followed by the DRR, *k*-NN, and LCC. However, BioCLUST produced higher bias than both DRR and *k*-NN. The general conclusion of the comparison was that the overall choice of method rests on both the availability of data sets and the level of precision required. The BioCLUST method provides practical advantages when geo-referenced plot data are not available on a scene-specific basis, however, implementation requires the availability of a stand-level photo-inventory for at least a representative portion of the satellite image.

[2] Labrecque, S., Fournier, R.A., Luther, J.E., Piercey, D.E., A comparison of four methods to map forest biomass from Landsat-TM and inventory data in western Newfoundland, manuscript under review, July 2005.

5. Summary and conclusions

The BioCLUST method uses a combination of forest type and structure information derived from Landsat TM imagery and stand-level regression equations derived from regional field plots to map forest biomass. BioCLUST was tested at both pixel and landscape scales with the following main conclusions:

(i) The discrimination of broad forest cover classes (coniferous, broadleaf, and mixed forest types) showed good agreement with field plots and the forest management photo-inventory, with overall classification accuracies of 77 and 74%, respectively. However, there was poor discrimination of forest species types (e.g., bF-, bS-, Hs-, Sh-, or wB-dominated), with overall accuracies less than 50%.

(ii) Validation of the biomass estimates showed RMSE values ranging from 43 to 79 tonnes/ha, with lower errors for the broadleaf-dominant classes and higher errors for the mixed forest classes. RMSE values were lower for intermediate height classes, with increasing RMSE values for the higher height classes.

(iii) The BioCLUST method overestimated biomass for the low height and open stands (i.e., low biomass) and underestimated biomass for the higher height and dense crown closure stands (i.e., high biomass), suggesting a limitation in the range of biomass values that could be mapped. Overall bias was negative at 10 tonnes/ha compared with a negative bias of 3 tonnes/ha estimated for the photo-inventory.

(iv) Landscape-level validation gave lower overall RMSE values than the field plot assessment (37–47 tonnes/ha), however, the errors inherent in the photo-inventory biomass are not accounted for at this level. Overall landscape biomass estimates were within 0.4% of biomass mapped using the forest management photo-inventory of the study area.

(v) BioCLUST offers an alternative to other biomass mapping methods when scene-specific plot data are limited and a photo-inventory is available for a representative portion of the satellite scene.

Acknowledgements

This study was made possible by the generous support of the Newfoundland Department of Forest Resources and Agrifoods in sharing their inventory data. In particular, we extend our thanks to Darrell Harris, Boyd Pittman, Scott Payne, and Paul White. We also thank our Canadian Forest Service colleagues, André Beaudoin, Chun-Huor Ung, Pierre-Yves Bernier, Marie-Claude Lambert, Eric Arsenault, and Guy Strickland for their attention and assistance on this project. This research project is included in the Earth Observation for Sustainable Development of Forests (EOSD) project supported jointly by the Canadian Space Agency and Natural Resources Canada, Canadian Forest Service. Earlier development of this work was made possible by a grant (project P-476 LA-98-10) from the Energy from the FORest (ENFOR) program of Natural Resources Canada, Government of Canada.

References

Bauer, M.E., Burk, T.E., Ek, A.R., Coppin, P.R., Lime, S.D., Walsh, T.A., Walters, D.K., Befort, W., Heinzen, D.F., 1994. Satellite inventory of Minnesota forest resources. Photogr. Eng. Rem. Sens. 60 (3), 287–298.

Beaudoin, A., Guindon, L., Leboeuf, A., Luther, J.E., Ung, C.H., Côté, S., Lambert, M.-C., 2005. Biomass mapping of Canadian northern boreal forests using a *k*-NN approach and sample plots from high resolution QuickBird images. In: Proceedings, 26th Canadian Symposium on Remote Sensing, Wolfville, Nova Scotia, June 14–16.

Bonnor, G.M., 1985. Inventory of Forest Biomass in Canada. Nat. Res. Can., Can. For. Serv.-Petawawa National Forestry Institute, Petawawa, Ontario.

Brown, S.L., Schroeder, P., Kern, J.S., 1999. Spatial distribution of biomass in forests of the eastern USA. For. Ecol. Manage. 123, 81–90.

Canadian Council of Forest Ministers, 1997. Criteria and Indicators of Sustainable Forest Management in Canada. Canadian Council of Forest Ministers, Ottawa, Ontario.

Carpenter, G.A., Gjaja, M.N., Gopal, S., Woodcock, C.E., 1997. ART neural networks for remote sensing, vegetation classification from Landsat TM and terrain data. IEEE Trans. Geosci. Rem. Sens. 35 (2), 308–325.

Cohen, W.B., Maiersperger, T.K., Spies, T.A., Oetter, D.R., 2001. Modelling forest cover attributes as continuous variables in a regional context with Thematic Mapper data. Int. J. Rem. Sens. 22, 2279–2310.

Cohen, W.B., Spies, T.A., 1992. Estimating structural attributes of Douglas-fir/western hemlock forest stands from Landsat and SPOT imagery. Rem. Sens. Environ. 41, 1–17.

Congalton, R.G., 1991. A review of assessing the accuracy of classifications of remotely sensed data. Rem. Sens. Environ. 37, 35–46.

Damman, A.W.H., 1983. An ecological subdivision of the island of Newfoundland. In: South, G.R. (Ed.), Biogeography and Ecology of the Island of Newfoundland. Monographiae Biologicae 48. Dr. W. Junk Publishers, The Hague, Netherlands, pp. 163–206.

Delaney, B.B., Osmond, S.M., 1977. The Forest Management Inventory of Newfoundland. Report to the Department of Forestry and Agriculture, FI-5.

Dong, J., Kaufmann, R.K., Myneni, R.B., Compton, J.T., Kauppi, P.E., Liski, J., Buermann, W., Alexeyev, B., Hughes, M.K., 2003. Remote sensing estimates of boreal and temperate forest woody biomass carbon pools, sources, and sinks. Rem. Sens. Environ. 84, 393–410.

Fang, J., Wang, G., Liu, G., Xu, S., 1998. Forest biomass of China: an estimate based on the biomass–volume relationship. Ecol. Appl. 8, 1084–1091.

Fazakas, Z., Nilsson, M., Olsson, H., 1999. Regional forest biomass and wood volume estimation using satellite and ancillary data. Agric. For. Meteorol. 98–99, 417–425.

Fournier, R.A., Luther, J.E., Guindon, L., Lamber, M.C., Piercey, D., Hall, R., 2003. Mapping aboveground tree biomass at the stand level from inventory information, test cases in Newfoundland and Quebec. Can. J. For. Res. 33, 1846–1863.

Franco-Lopez, H., Ek, A.R., Bauer, M.E., 2001. Estimation and mapping of forest stand density, volume, and cover type using the *k*-nearest neighbors method. Rem. Sens. Environ. 77, 251–274.

Gemmell, F.M., Varjo, J., 1999. Utility of reflectance model inversion versus two spectral indices for estimating biophysical characteristics in a boreal forest test site. Rem. Sens. Environ. 68, 95–111.

Hall, F.G., Knapp, D.E., Huemmrich, K.F., 1997. Physically based classification and satellite mapping of biophysical characteristics in the southern boreal forest. J. Geophys. Res. 102 (D24), 29567–29580.

Hall, F.G., Townshend, J.R.G., Engman, E.T., 1995. Status of remote sensing algorithms for estimation of land surface state parameters. Rem. Sens. Environ. 51, 138–156.

He, H.S., Mladenoff, D.J., Radeloff, V.C., Crow, T.R., 1998. Integration of GIS data and classified satellite imagery for regional forest assessment. Ecol. Appl. 8 (4), 1072–1083.

Kilpelainen, P., Tokola, T., 1999. Gain to be achieved from stand delineation in LANDSAT TM image-based estimates of stand volume. For. Ecol. Manage. 124 (2–3), 105–111.

Lavigne, M.B., 1982. Tree mass equations for common species of Newfoundland. Nat. Res. Can., Can. For. Serv.-Newfoundland and Labrador Region, St. John's, NL, Information Report N-X-213.

Lowe, J.J., Power, K., Gray, S.L., 1994. Canada's forest inventory 1991. Nat. Res. Can., Can. For. Serv.-Petawawa National Forestry Institute, Chalk River, ON, Information Report PI-X-115.

Lowe, J.J., Power, K., Gray, S.L., 1996a. Canada's forest inventory 1991. The 1994 Version. An addendum to Canada's forest inventory 1991. Nat. Res. Can., Can. For. Serv.-Pacific Forestry Centre, Victoria, BC, Information Report BC-X-362E.

Lowe, J., Power, K., Marsan, M., 1996b. Canada's forest inventory (1991). Summary by terrestrial ecozones and ecoregions. Nat. Res. Can., Can. For. Serv.-Pacific Forestry Centre, Victoria, BC, Information Report BC-X-364E.

Luther, J.E., Fournier, R.A., Hall, R.J., Ung, C.-H., Guindon, L., Piercey, D.E., Lambert, M.-C., 2002. A strategy for mapping Canada's forest biomass with Landsat TM imagery. Proc. Int. Geosci. Rem. Sens. Symp. (IGARSS '02)/24th Can. Symp. Rem. Sens. Toronto, Canada, 24–28 June (CD-ROM).

Mäkelä, H., Pekkarinen, A., 2004. Estimation of forest stand volumes by Landsat TM imagery and stand-level field-inventory data. For. Ecol. Manage. 196, 245–255.

Meades, W.J., Moores, L., 1994. Forest Site Classification Manual—A Field Guide to the Damman Forest Types of Newfoundland. Western Newfoundland Model Forest Inc., Corner Brook, NL, FRDA Report 003.

Nabuurs, G.J., Dolman, A.J., Verkaik, E., Kuikman, R.J., van Diepen, C.A., Whitmore, A.P., Daamen, W.P., Oenema, O., Dabat, P., Mohren, G.M.J., 2000. Article 3.3 and 3.4 of the Kyoto Protocol, consequences for industrialised countries' commitment, the monitoring needs, and possible side effects. Environ. Sci. Pol. 3, 123–134.

Newfoundland Forest Service, 1991. FORMAP Geographic Information System Database Catalogue. Government of Newfoundland and Labrador Department of Forestry and Agriculture.

Penner, M., Power, K., Muhairwe, C., Tellier, R., Wang, Y., 1997. Canada's forest biomass resources, deriving estimates from Canada's forest inventory. Nat. Res. Can., Can. For. Serv.-Pacific Forestry Centre, Victoria, BC, Info. Re BC-X-370.

Reese, H., Nilsson, M., Sandstrom, P., Olsson, H., 2002. Applications using estimates of forest parameters derived from satellite and forest inventory data. Comp. Electr. Agric. 37, 37–55.

Tomppo, E., Halme, M., 2004. Using coarse scale forest variables as ancillary information and weighting of variables in *k*-NN estimation: a genetic algorithm approach. Rem. Sens. Environ. 92, 1–20.

Woodcock, C.E., Collins, J.B., Gopal, S., Jakabhazy, V.D., Li, X., Macomber, S., Ryherd, S., Harward, V.J., Levitan, J., Wu, Y., Warbington, R., 1994. Mapping forest vegetation using Landsat TM imagery and a canopy reflectance model. Rem. Sens. Environ. 50, 240–254.

Wulder, M., Cranny, M., Dechka, J., 2002. An illustrated methodology for land cover mapping of forests with Landsat-7 ETM+ data, methods in support of EOSD land cover. Nat. Res. Can., Can. For. Serv.-Pacific Forestry Centre, Victoria, BC, Internal Report, Version 2.

Wulder, M.A., Dechka, J.A., Gillis, M.A., Luther, J.E., Hall, R.J., Beaudoin, A., Franklin, S.E., 2003. Operational mapping of the land cover of the forested area of Canada with Landsat data, EOSD land cover program. For. Chron. 79 (6), 1075–1083.